Cardiovascular Research (2016) **109**, 228–239
doi:10.1093/cvr/cvv266

Integrative miRNA and whole-genome analyses of epicardial adipose tissue in patients with coronary atherosclerosis

Michele Vacca[1,2,3†], Marco Di Eusanio[4‡], Marica Cariello[1,5], Giusi Graziano[1,5], Simona D'Amore[1,2,5], Francesco Dimitri Petridis[4], Andria D'orazio[2], Lorena Salvatore[2], Antonio Tamburro[2], Gianluca Folesani[4], David Rutigliano[6], Fabio Pellegrini[2], Carlo Sabbà[1], Giuseppe Palasciano[1], Roberto Di Bartolomeo[4], and Antonio Moschetta[1,2,5*]

[1]Department of Interdisciplinary Medicine, University of Bari 'Aldo Moro', Piazza Giulio Cesare 11, 70124 Bari, Italy; [2]Fondazione Mario Negri Sud, Santa Maria Imbaro (CH), Italy; [3]Ageing Research Center (CeSI), 'G. d'Annunzio' University Foundation, Chieti, Italy; [4]Cardiovascular Department, 'S.Orsola Malpighi' Hospital, University of Bologna, Bologna, Italy; [5]National Cancer Research Center IRCCS 'Giovanni Paolo II', Bari, Italy; and [6]Unit of Cardiology, 'San Paolo' Hospital, Bari, Italy

Received 1 May 2015; revised 1 November 2015; accepted 14 November 2015; online publish-ahead-of-print 8 December 2015

Time for primary review: 12 days

Background Epicardial adipose tissue (EAT) is an atypical fat depot surrounding the heart with a putative role in the development of atherosclerosis.

Methods and results We profiled genes and miRNAs in perivascular EAT and subcutaneous adipose tissue (SAT) of metabolically healthy patients without coronary artery disease (CAD) vs. metabolic patients with CAD. Compared with SAT, a specific tuning of miRNAs and genes points to EAT as a tissue characterized by a metabolically active and pro-inflammatory profile. Then, we depicted both miRNA and gene signatures of EAT in CAD, featuring a down-regulation of genes involved in lipid metabolism, mitochondrial function, nuclear receptor transcriptional activity, and an up-regulation of those involved in antigen presentation, chemokine signalling, and inflammation. Finally, we identified miR-103-3p as candidate modulator of CCL13 in EAT, and a potential biomarker role for the chemokine CCL13 in CAD.

Conclusion EAT in CAD is characterized by changes in the regulation of metabolism and inflammation with miR-103-3p/CCL13 pair as novel putative actors in EAT function and CAD.

Keywords Epicardial adipose tissue • Gene expression • miRNA • Metabolic syndrome • Nuclear receptors

1. Introduction

Epicardial adipose tissue (EAT) thickness and volume strongly reflect obesity, intra-abdominal visceral fat, and insulin resistance.[1,2] Indeed, EAT thickness is an independent risk factor for coronary artery disease (CAD), atrial fibrillation, and other cardiac diseases.[3–5] EAT surrounds heart muscle and coronary arteries, and shares with these organs the same microcirculation.[6] EAT vascularization is supplied by branches of the coronary arteries, and no muscle fascia divides EAT from the myocardium.[7] Under physiological conditions, different metabolic, cardioprotective, and thermogenic ('brown-like') functions have been attributed to EAT,[1,8] that can vary depending on EAT anatomical location.[9] A substantial inflammatory infiltrate has been described in EAT, since EAT produces several bioactive molecules, including pro-inflammatory cytokines[9–12] that could be paracrinally or vasocrinally secreted to the myocardium and to the coronary artery wall. EAT could thus be able to modulate heart and coronary artery physiology,[13] and mounting evidences point to EAT as a candidate player in pathophysiology of CAD and cardiac disease.[1,13]

miRNAs are small, non-coding RNAs acting as fine post-transcriptional tuners of gene expression, either interfering with

* Corresponding author. Tel: +39 0805593262; fax: +39 0805555388, E-mail: antonio.moschetta@uniba.it

† M.V. is currently Senior Clinician Scientist at the Medical Research Council Human Nutrition Research (MRC-HNR), and research fellow at the Institute of Metabolic Science, University of Cambridge, UK.

‡ M.D.E. is currently Director of the Cardiac Surgery Unit, Cardiovascular Department, 'Giuseppe Mazzini' Hospital of Teramo, Italy.

protein translation or reducing transcript levels.[14] miRNAs act on multiple targets and complex pathways, thus representing candidate regulators of metabolic homeostasis, adipocyte differentiation, AT function, and inflammation.[15] miRNAs have also been described as differentially modulated in adipose tissue during metabolic disease, thus being considered candidate biomarkers for metabolic disease and CAD, and putative targets for therapy.[16,17]

In the present study, we depicted a comparative miRNA and whole-genome expression chart from EAT and subcutaneous adipose tissue (SAT) in 'metabolically healthy' patients without CAD and in metabolic patients with CAD. This strategy allowed us to identify a set of genes/miRNA characterizing EAT in health and disease as well as novel biological processes characterizing EAT in CAD. Also, we characterized CCL13/MCP4 as a putative biomarker of CAD.

2. Methods summary

Forty-four Caucasian male patients were recruited at the University of Bologna; 15 underwent cardiac valve surgery (CTRL group; no history/evidences of CAD/carotid atherosclerosis; <1 criterion for Metabolic Syndrome, MS), and 29 underwent coronary artery bypass graft surgery (CAD group). Gene/miR microarray expression analyses were conducted on RNA extracted from SAT and perivascular EAT using the 'Illumina HumanHT-12-V3' and 'Human-V2-MicroRNA' Expression Kits (Illumina iScan). Data were processed using Illumina Genome Studio, SAS software, and R package. Differentially expressed genes were studied using Ingenuity Pathway Analysis (Ingenuity System Inc., USA). Microarray data are available on GEO (Ref: GSE64566; http://www.ncbi.nlm.nih.gov/geo/query/acc.cgi?acc=GSE64566). Quantitative PCR confirmations were performed to validate genes (High Capacity DNA Archive Kit and Power Sybr Green, Applied Biosystem) and miRNAs (TaqMan miRNA Assays, Applied Biosystems). Formalin-fixed adipose tissue specimens were used for H&E and IF. Circulating RANTES and MCP-4 in the serum were determined by commercially available ELISA kits (RayBiotech, Inc.). Microarray analysis was performed in 23 subjects; RT–qPCR confirmations in 41 subjects; IF in 14 subjects; serum cytokine analysis in 43 subjects plus an external validation cohort (19 subjects) of patients with risk factors of CAD (Study design in Supplementary material online, *Figure S1*). Human heart pre-adipocytes (HPAd) and human kidney (HEK-293) cells were obtained from Public Health England (PHE) and American Type Tissue Collection (ATTC), respectively. HPAd cells were differentiated following manufacturer's instructions. miRIDIAN hsa-miR-103 mimic and hairpin inhibitor, or negative controls (Thermo Scientific) were transfected using Lipofectamine LTX following manufacturer's instructions (Invitrogen) in differentiated adipocytes. 3′UTR Luciferase Reporter Assay was performed using HEK-293 cells, hsa-miR-103 mimic and hairpin inhibitor, or negative controls, together with 3′UTR or 3′UTR mutant (deletion of miR-103 target sequence) provided by Genecopoeia. Luciferase activity (Firefly/Renilla luciferase ratio) was measured using the Dual-Glo Luciferase Assay (Promega). Detailed experimental procedures are provided in the Supplementary material.

3. Results

3.1 Study population

We enrolled 29 CAD patients (93% with MS) and 15 'controls' (CTRL), namely subjects undergoing cardiac valve replacement ($n = 15$, with ≤1 Adult Treatment Panel III–ATPIII criteria for MS) with negative clinical and instrumental evidences of atherosclerosis and CAD. Compared with 'controls', CAD patients were characterized by significantly increased abdominal circumference (AC), BMI, systolic blood pressure, heart rate, glycaemia, and systemic inflammation, while HDL-c was decreased. Characteristics of the study population are provided in Supplementary material online, *Table S1A* and *B*.

3.2 A specific gene expression matrix characterizes EAT from SAT

To measure the gene expression patterns that characterize EAT from SAT, we used the whole-genome microarrays. Overall, the signal intensity of 1131 genes resulted statistically different at the Wilcoxon signed-rank test in EAT (vs. SAT), thus underscoring the profound diversity of EAT and SAT. To depict atherosclerosis-independent and -dependent peculiarities of EAT vs. SAT, we selected 421 annotated genes (*Figure 1A*; 173 down-regulated, see Supplementary material online, *Table S2B*; 248 up-regulated, see Supplementary material online, *Table S2D*) that were significantly different (EAT vs. SAT) in the overall population ($P < 0.01$; FDR < 0.01) and at least in one of the two subgroups (CTRL or CAD; Cut-off: $P < 0.05$, fold change > 1.5). To provide a framework for interpretation of our results, we then functionally clustered significant biological pathways using the Core Function of Ingenuity System Pathway Analysis (IPA; see Supplementary material online, *Table S2A* and *C*). We considered 'biologically relevant' only those 'statistically significant' items included in 'significantly modulated' pathways.

EAT profiling revealed a clear 'inflammatory scenario' both in CTRL and in CAD, as confirmed by the up-regulation of pro-inflammatory pathways, macrophage surface antigens (CD14 and CD163), and cytokines. In addition to the up-regulation of inflammatory mediators previously described in EAT of CAD subjects (i.e. IL6; chemoattractant protein-1, MCP-1; CCL5/RANTES; intercellular adhesion molecule 3, ICAM3/CD50; chemokine C-C motif ligand 8, CCL8/MCP-2; 'neutrophil chemotactic factor' IL8; CCL21/6Ckine; chemokine C-X-C motif ligand 2, CXCL2; IL-7 receptor, IL-7R),[9–12,18,19] we also profiled an increase of other key players in inflammation (e.g. CCL13/MCP-4; toll-like receptor 5, TLR5), and VEGFC. Pro-inflammatory signals were more prominent in CAD patients, while reduced 'extracellular matrix deposition and fibrosis', inhibition of the oxysterol sensor Liver X Receptor (LXR), and Phosphatase and Tensin Homologue (PTEN) activation were more prominent in the EAT of the CTRL group.

Using the Random Forest (RF) algorithm, we then studied the ability of our set of genes to characterize EAT from SAT. RF is able to 'score', in order of 'relative importance' (RI, see Supplementary material online, *Table S2B* and *D*), the capability of each variable to distinguish two specific conditions. According to RF, 14 differentially modulated genes (EAT vs. SAT; *Figure 1B*) characterize the 'identity card' of EAT from SAT independently from patients' disease. This list features 4 up-regulated and 10 suppressed genes. Indeed, the accuracy of these genes in distinguishing EAT from SAT has been estimated by the algorithm as high as 100% (C-Index = 1; *Figure 1C*).

Overall, we provided a comprehensive CAD-independent gene expression signature of EAT vs. SAT, and we showed that increased inflammatory signals are not necessarily associated to the concomitant presence of CAD. These features sustain the novel concept that inflammation is required for a proper adipose tissue function,[20] and that the presence of inflammatory infiltrates as well as a generic over-activation of inflammatory signals not necessarily predict the presence of disease.

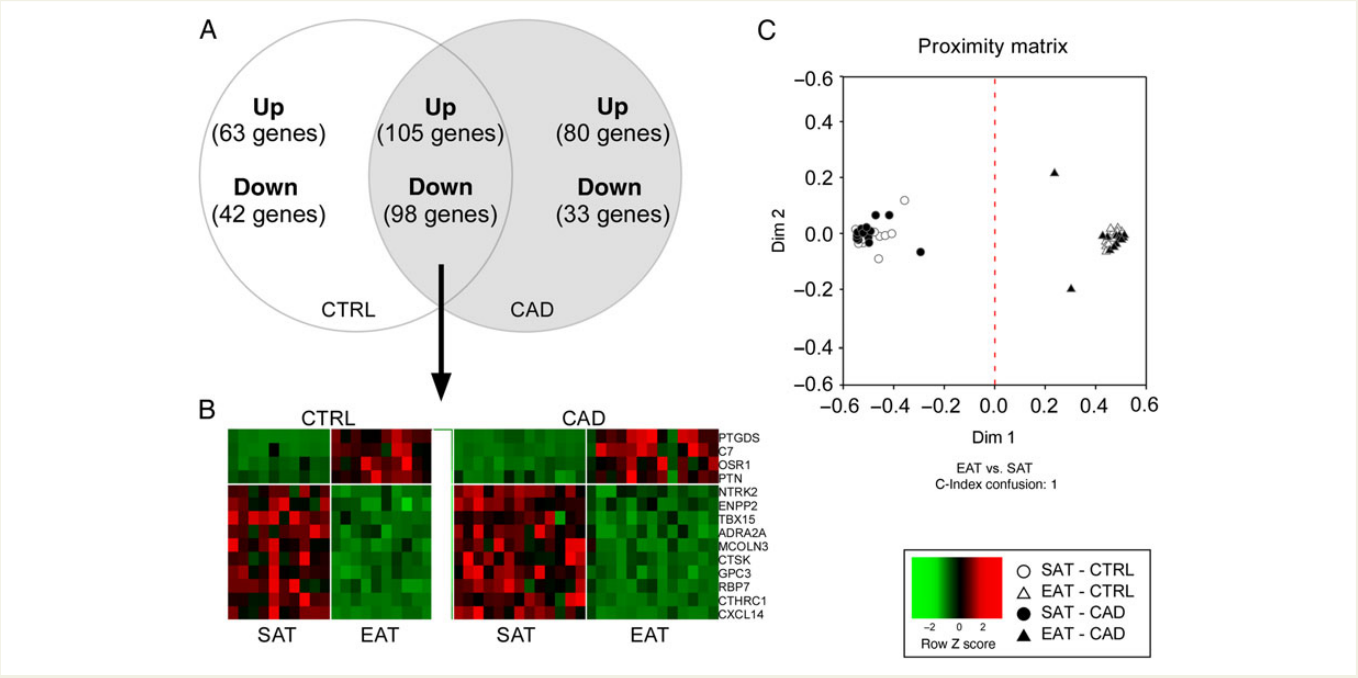

Figure 1 GE 'identity card' of EAT vs. SAT. (*A*) Genes expression patterns characterizing EAT vs. SAT (*n*: 23; 10 CTRL and 13 CAD for both EAT and SAT). Of the 421 genes differentially regulated (EAT vs. SAT), 203 genes showed a common pattern of expression (CTRL and CAD patients). RF analysis identified 14 genes (*B*) with RI $>$ 0.5 that discriminate EAT from SAT independently from patients' disease. (*C*) Proximity matrix (RF algorithm): on the basis of the levels of expression of these 14 genes, RF discriminates EAT from SAT with 100% accuracy (C-Index = 1). Data are shown in a heatmap with a matrix format of the genes differentially modulated; single rows represent gene expression in a single patient (column). Colours: red, expression greater than the mean; black, expression equal to the mean; green, expression smaller than the mean. Detailed results are given in Supplementary material online, *Table S2*.

3.3 A specific miRNA expression matrix characterizes EAT from SAT

The second step was to define the miRNome characterizing EAT vs. SAT in the overall population. In the entire study group samples, 6 miRNAs were significantly up-regulated and 19 down-regulated in EAT vs. SAT (Wilcoxon signed-rank test, $P \leq 0.01$; FDR ≤ 0.1; fold change $>$ 1.5 in CTRL or CAD subgroup; *Figure 2A* and see Supplementary material online, *Table S3*). In the up-regulated miRNAs, of particular interest is miR-146b-5p known to promote adipogenesis.[15] Five miRNAs were significantly down-regulated in the overall population and in both subgroups of patients (CTRL and CAD; *Figure 2B*), thus being characteristic of EAT vs. SAT, independently from the presence of CAD. These EAT-specific miRNAs are miR-196b-5p, miR-196a-5p (a promoter of brown adipogenesis[21]), miR-18a-3p (a member of the miR-17/92 cluster that promotes adipocyte differentiation[22]), and miR-10a-3p (an anti-inflammatory agent[23]). Some of these miRNAs could coordinately sustain the pro-inflammatory profile emerged from the whole-genome analysis; for example, we profiled a suppression of the anti-inflammatory miR-10a-3p and miR-23a-5p that have been shown to target monocyte chemotactic protein 1 (MCP-1), IL6, and IL8[23,24] (up-regulated in EAT vs. SAT).

According to RF, the differential modulation of miR-196a-5p and miR-19b-5p is highly specific for EAT (see Relative Importance, RI, in Supplementary material online, *Table S3* and patterns of expression in *Figure 2B*), and the levels of expression of these two miRNAs characterize EAT with an accuracy of 74% (C-Index = 0.74; *Figure 2C*).

Overall, we were able to depict a novel miRNA signature of EAT vs. SAT characterized by an up-regulation of miRNAs that are able to promote adipogenesis (miR-146b-5p) and a suppression of anti-inflammatory miRNAs (miR-23a-5p and miR-10a-3p).

3.4 A specific microRNA matrix characterizes EAT in CAD

We then characterized CAD-specific miRNA expression changes in EAT. Compared with CTRL group, the expression patterns of 15 miRNAs appeared to be significantly up-regulated (Mann–Whitney *U* test, $P < 0.05$; FDR ≤ 0.3; fold change $>$ 1.2), while 14 miRNAs down-regulated (*Figure 3A* and see Supplementary material online, *Table S4A,B*; Changes in SAT for comparison are reported in Supplementary material online, *Table S4 C* and *D*). In EAT of CAD patients, we found increased miR-135b-3p (a direct target of inflammatory pathways[25]), while Let-7a-3p and miR-127-3p (negative modulators of inflammatory pathways[16,26]) were down-regulated. In EAT of CAD patients, we also found suppressed miR-455-3p (a driver of during brown adipocyte differentiation[27]), miR-193b-3p (promoting adiponectin secretion in human adipocytes),[28] miR-30a-5p and miR-103-3p (but not of miR-103-3p paralogous miR-107, see qPCR confirmation in Supplementary material online, *Figure S2C*). miR-30a-5p and miR-103-3p are considered key players in white adipose tissue differentiation and function. Indeed, these miRNAs are induced during adipogenesis and can accelerate this process when ectopically overexpressed.[29,30] miR-30a-5p is known to be down-regulated in obesity,[29,31] while there

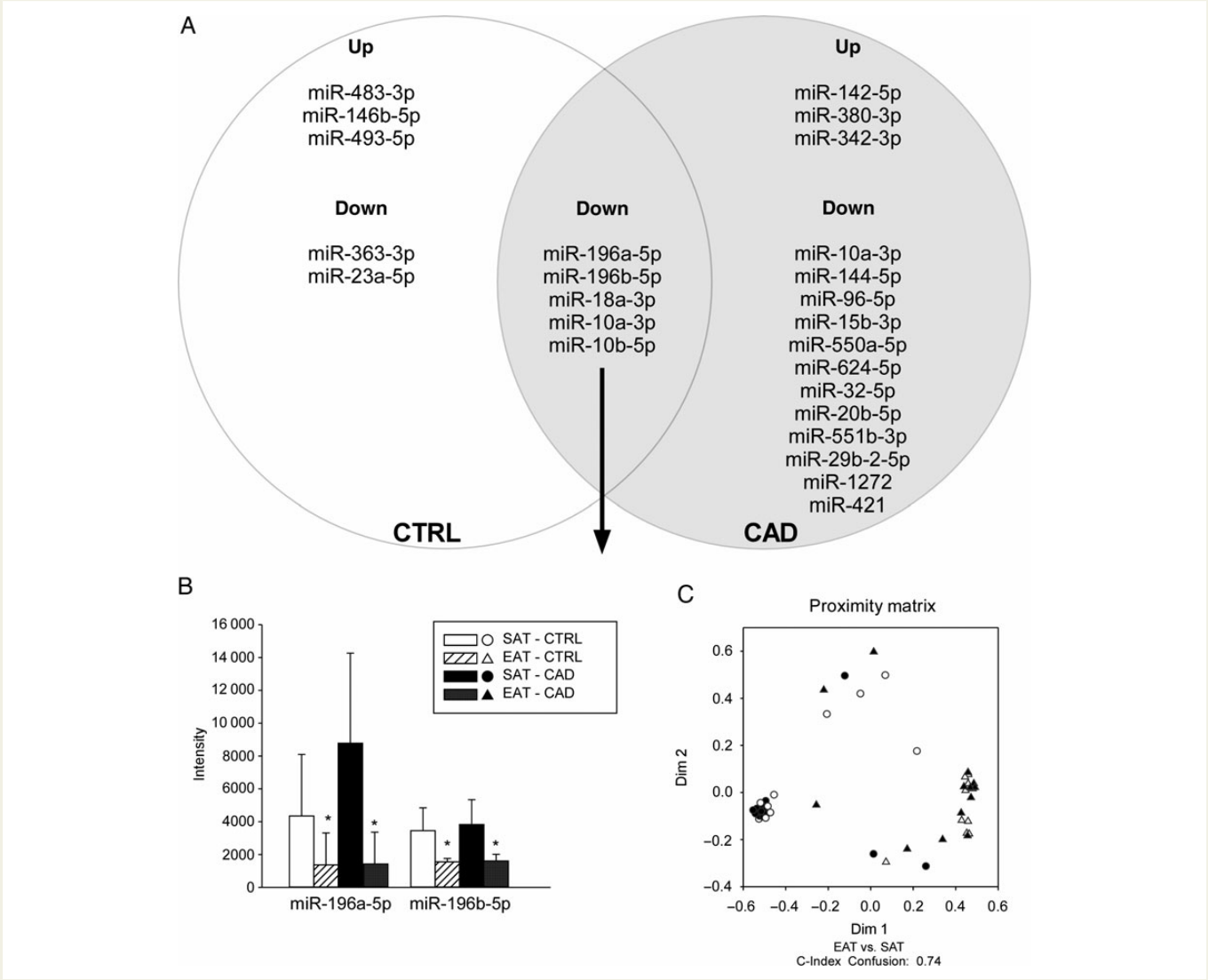

Figure 2 miRNA 'identity card' of EAT vs. SAT. (*A*) Changes in miRNA expression patterns characterizing EAT vs. SAT (*n*: 23; 10 CTRL and 13 CAD for both EAT and SAT). Of the 25 miRNA differentially regulated in EAT vs. SAT, 5 miRNAs showed a common pattern of suppression in CTRL and CAD patients. RF analysis identified miRNA 196a-5p and 196b-5p as the items with the best discriminating potential (*B*) independently from patients' disease. (*C*) Proximity matrix of the RF algorithm: on the basis of the levels of expression of 196a-5p and 196b-5p, RF discriminates EAT from SAT with an accuracy of 74% (C-Index = 0.74). Data are shown as mean ± SD, and statistical significance assessed with Wilcoxon signed-rank test. Detailed results are provided in Supplementary material online, *Table S3*.

is no agreement with regard to miR-103-3p expression changes (see below). We confirmed the differential changes of miR-30a-5p, miR-103-3p, miR-135b-3p, and miR-651-5p by RT–qPCR (*Figure 3B*) in the expanded population and analysed our data with the RF algorithm: although not massively differentially modulated, changes in these miRNAs predict the 'CAD status' with a high accuracy (C-Index: 0.75, *Figure 3C*).

We thus provided the evidence that patients with CAD present differentially modulated EAT-specific miRNA expression patterns. Since candidate miRNAs are considered players in inflammation (i.e. miR-135b-3p, miR-193b-3p, and Let-7a-3p) and adipocyte function (i.e. miR-455-3p, miR-30a-5p, and miR-103-3p), our data elect these miRNAs as putative actors in the pathophysiological events characterizing EAT inflammation in MS, as well as their potential involvement in CAD.

3.5 Repression of metabolic and RXR-heterodimer pathways is distinctive of CAD in EAT

We then characterized a matrix of EAT gene pathways suppressed in CAD. The signal intensity of 89 genes were significantly down-regulated in CAD patients (Mann–Whitney *U* test, $P < 0.05$; FDR $\leq$ 0.2; fold change > 1.2 vs. CTRL; *Figure 4A* and see Supplementary material online, *Table S5B*. Changes in SAT for comparison are reported in Supplementary material online, *Figure S3* and detailed in Supplementary material online, *Table S5C* and *D*). Both IPA pathway analysis (see Supplementary material online, *Table S5A*) and IPA 'upstream regulator' prediction tool [that predicts the status of activation of a specific modulator (e.g. a transcription factor) on the basis of the differential modulation of its known targets; *Figure 5A*] featured a down-regulation of the

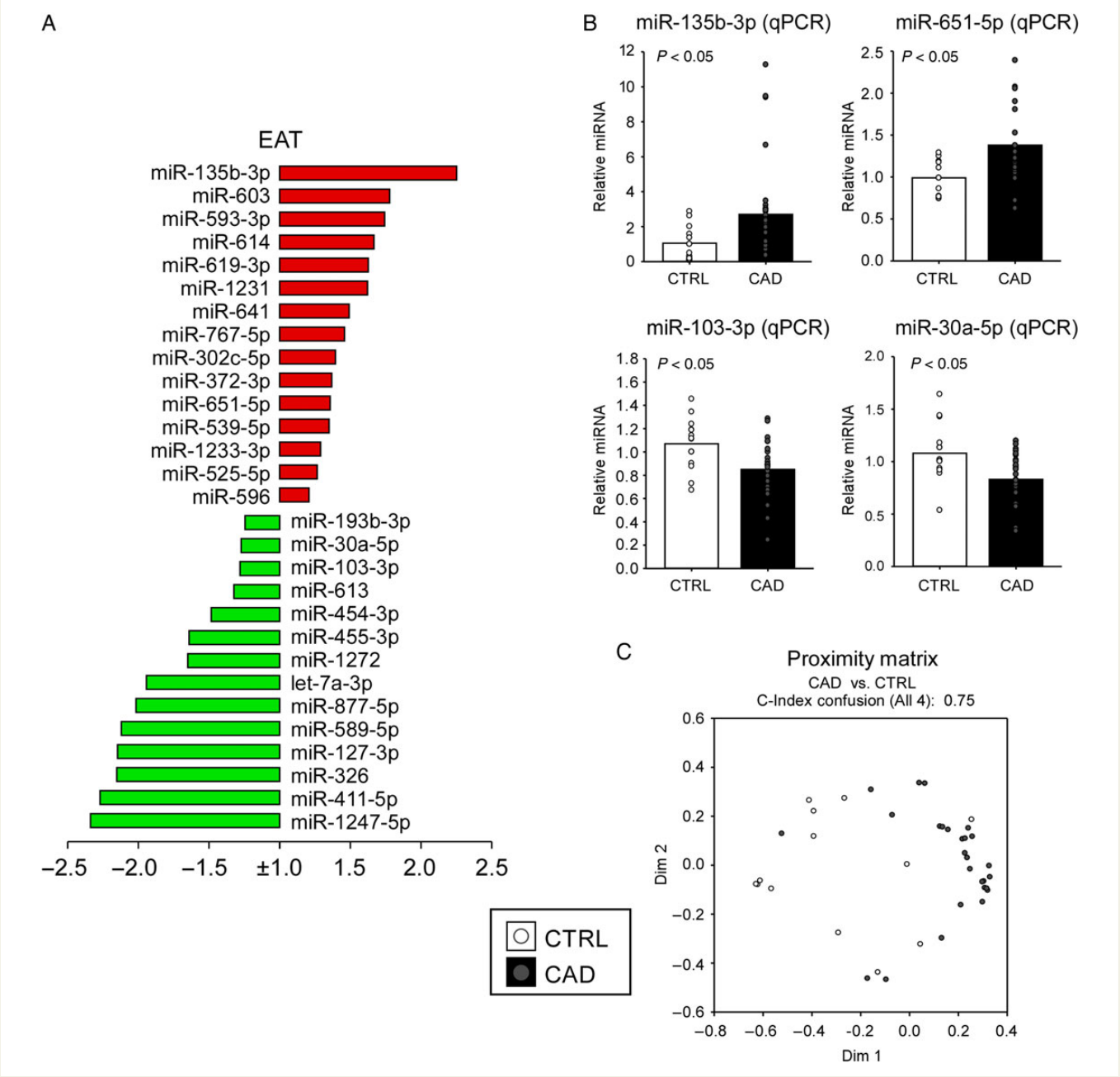

Figure 3 miRNAs profiling in EAT of CAD patients. (*A*) Changes in miRNA expression patterns characterizing EAT of CAD patients (vs. controls) are shown as lateral bars representing fold changes among groups (detailed results are provided in Supplementary material online, *Table S4A* and *B*). (*B*) RT–qPCR confirmations (13 CTRL vs. 28 CAD patients): relative mRNA expression levels of miR-135b, miR-651, miR-103, and miR-30a. U6snRNA was used as reference (housekeeping) miRNA, and values were normalized to data obtained from EAT of CTRL group. Means are represented as bars; variability among patients is represented with a scatter plot (•patient). Statistical significance ($P \leq 0.05$) was assessed by Mann–Whitney rank sum test. (*C*) Proximity matrix of the RF algorithm: on the basis of the levels of mRNA expression of miR-135b3p, and miR-651, miR-103, and miR-30a, RF discriminates controls from CAD patients in 75% of cases (C-Index = 0.75).

metabolic pathways related to adipose tissue function (glycerolipid and fatty acid metabolism, oxidative phosphorylation, mitochondrial function), as a consequence of a suppressed transcriptional activity of lipid-sensing nuclear receptors (NRs; peroxisome proliferator-activated receptors, PPARs; liver X receptors, LXRs; retinoid X receptor alpha, RXRα; retinoid acid receptors, RAR) and of other transcription factors involved in the regulation of metabolism (e.g. Forkhead box protein O1, FOXO1; sterol regulatory element-binding protein 1, SREBP-1).

The signature of a reduced lipid- and retinoid-sensor NRs featured a reduced mRNA expression of RXRα and of their target genes lipoprotein lipase[32,33] and adenylate cyclase (ADCY3 and ADCY6), PTEN, retinol dehydrogenase 14 (RDH14), zinc finger and BTB domain containing 16 (ZBTB16), and SWI/SNF-related, matrix-associated, actin-dependent regulator of chromatin, subfamily d, member 2 (SMARCD2). Interestingly, also miR-103-3p is included in the suppressed interactome, since it is a confirmed target of PPARγ,[34]

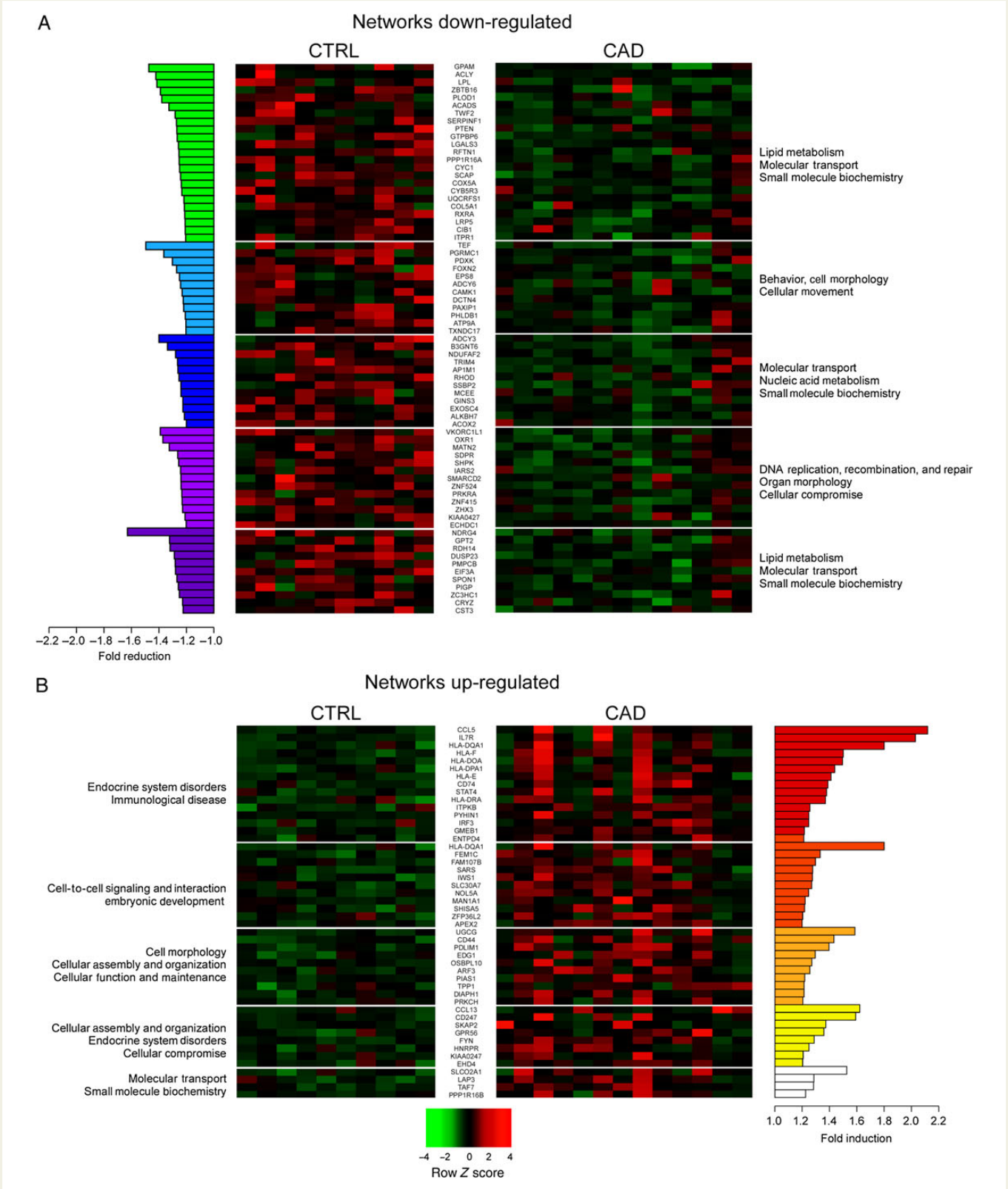

Figure 4 Gene expression profiling in EAT of CAD patients. Genes down- (*A*) and up-regulated (*B*) in EAT (*n*: 13) of CAD patients (vs. CTRL, *n*: 10) were profiled using microarrays, and clustered in large networks displaying a coordinate biological function. Data are shown in a heatmap with a matrix format of the genes differentially modulated within the specific network; single rows represent gene expression in a single patient (column). Colours: red, expression greater than the mean; black, expression equal to the mean; green, expression smaller than the mean. Lateral bars: fold changes among groups. Detailed results are given in Supplementary material online, *Tables S5A,B* and *S6A,B*.

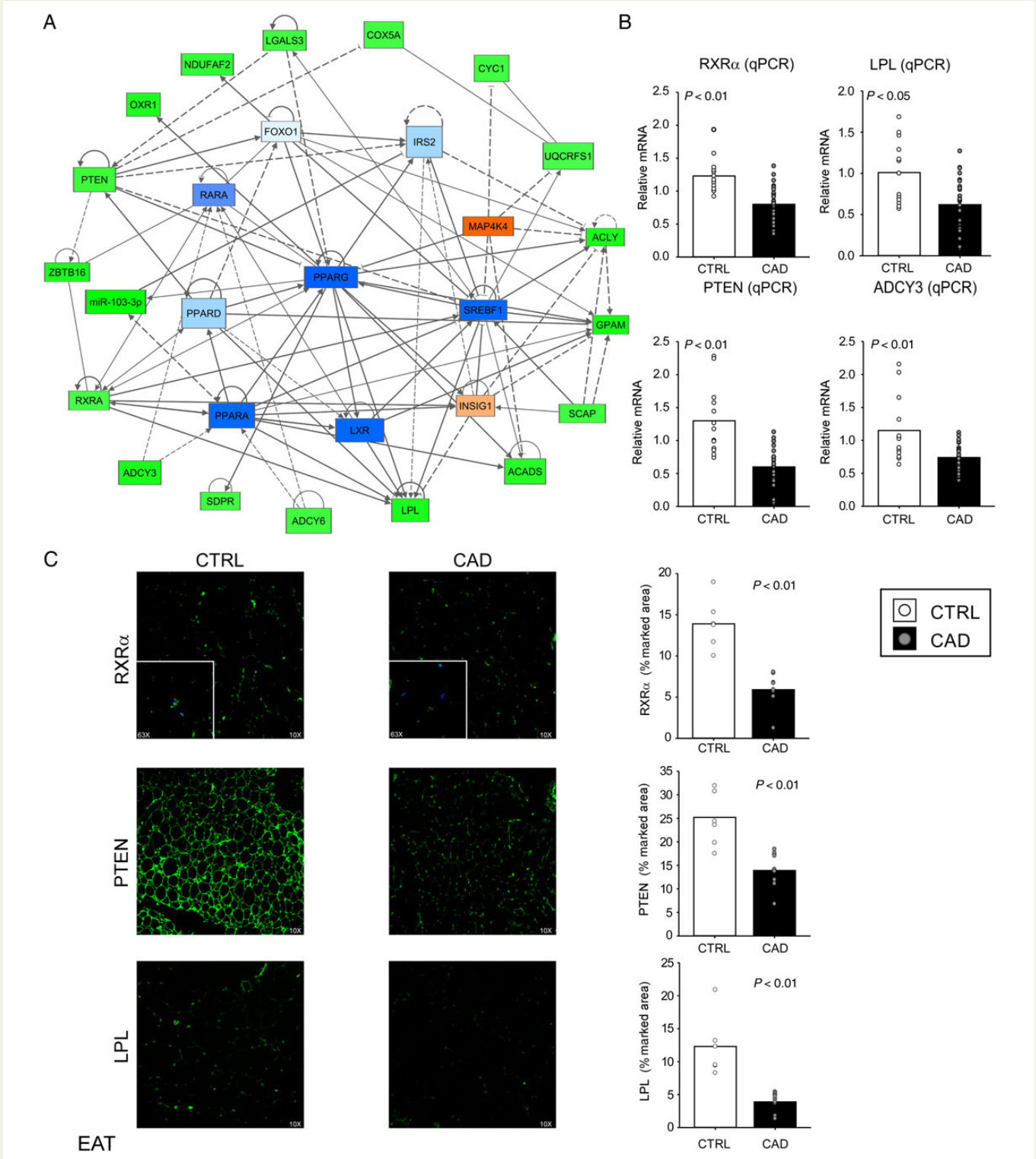

Figure 5 EAT of CAD patients is characterized by a reduced activation of lipid-sensing and retinoid-sensing NRs. (*A*) IPA 'upstream regulators' prediction tool reveals, on the basis of the genes suppressed (green) in EAT (CAD vs. CTRL), the suppression of lipid- and retinoid-sensing transcription factors (in blue; even if not modulated at RNA level), and an up-regulation of INSIG1 and MAP4K4 (in orange); intensity of colour represents the magnitude of the predicted regulation, dashed arrows indirect relationships or relationships not fully supported. (*B*) RT–qPCR confirmations (13 CTRL vs. 28 CAD patients): relative mRNA expression of RXRα, LPL, PTEN, and ADCY3. GAPDH was used as reference gene, and values were normalized to data obtained from CTRL patients. Means are represented as bars; variability among patients is represented with a scatter plot (•: patient). (*C*) IF (6 CTRL vs. 8 CAD patients) provides the evidence that RXRα, LPL, PTEN proteins are reduced in EAT of CAD patients (% of marked area quantified using the ImageJ software). Statistical significance ($P \leq 0.05$) was assessed by the unpaired Mann–Whitney rank sum test.

predicted as inhibited on the basis of its downstream targets. We confirmed the suppression of the most represented genes in the pathway analysis (RXRα, LPL, and PTEN) in EAT of CAD patients (transcript by RT–qPCR and of proteins by IF; *Figure 5B* and *C*, respectively). These molecular patterns point to an intriguing down-regulation of genes involved in lipid metabolism, mitochondrial function, and lipid- and retinoid-sensing NR transcriptional activation in EAT of patients with CAD. These findings are of particular interest since: (i) NRs transcription factors act as key players in the modulation of metabolic homeostasis, inflammation, and circadian rhythms, and could influence cardiometabolic disease and pro-inflammatory signals in EAT;[35,36] (ii) EAT has been described as an active metabolic tissue exhibiting 'beige' features[8]; (iii) the presence of CAD has been associated to a 'brown-to-white' adipocyte transdifferentiation in EAT.[37]

3.6 Increased immune responses are distinctive of EAT in CAD

We also profiled 57 significantly (Mann–Whitney *U* test, $P < 0.05$; FDR ≤ 0.2; fold change > 1.2) up-regulated genes in EAT of CAD patients. The overexpressed interactome provided the evidence of an activation of both innate and adaptive immune responses in CAD, with an up-regulation of the MHC class II molecules (high-fat diet-induced MHC class II overexpression promotes macrophage accumulation in adipose tissue, and pro-inflammatory M1 polarization,[38,39] while the deletion of MHC II leads to reduced accumulation of macrophages in the AT, improves insulin sensitivity, and protects form diet-induced obesity complications[40]), an enhanced cross-talk among immune-modulatory cells, and a strong up-regulation of inflammatory cell growth, recruitment, and activity (details in *Figure 4B* and in Supplementary material online, *Table S6A,B*; for comparison, SAT data in Supplementary material online, *Figure* S3 and *Table S6C,D*). EAT is thus a source of mediators that could accumulate and retrieve monocytes in EAT and in the intima to differentiate into macrophages, a critical step in the development of the atherosclerotic plaque.[41] These genomic features support previous reports showing more pro-inflammatory EAT infiltrates in the CAD vs. CTRLs.[12,42,43] These results are of a particular value since atherosclerotic lesions develop mainly in the coronary arteries surrounded by fat, and EAT quantity and macrophage infiltration have been related to atherosclerotic plaque size and composition.[44]

We thus provided the evidence of a complex over-activation of the inflammatory cascades in EAT of CAD patients at transcriptional level, pointing to the antigen presenting pathways (MHC Class II), the enhanced communication among inflammatory cells, and chemokine signalling (CCL5, CCL13, and CCL5R) as prominent features. This CAD-specific EAT profile could induce or, at least, sustain the systemic inflammatory response, and potentially promote coronary atherosclerosis.

3.7 Enhanced production and release of chemokines CCL5 and CCL13 in EAT of CAD patients

Given the prominent inflammatory profile characterizing EAT vs. SAT, we specifically focused on the inflammatory cytokines Chemokine C–C motif ligand 5 (CCL5/RANTES) and 13 (CCL13/MCP-4) that were the only chemokines increased in EAT of CAD patients (vs. controls). IPA also predicted CCR5 (CCL5 and CCL13 receptor) signalling as activated in EAT of CAD patients (vs. controls). The overexpression of these chemokines was confirmed by RT–qPCR in the expanded population (*Figure 6A* and *B*), and by IF (*Figure 6C* and *D*). A pro-atherogenic role has been highlighted for both these chemokines. CCL5 has been previously described overexpressed in EAT of overweight and CAD patients,[18,45] and its protein content is correlated positively to macrophage infiltration and inversely to calcification in the atherosclerotic plaque.[46] Although pathophysiologically very interesting for atherosclerosis plaque formation (CCL5 binds proteoglycans in the vascular walls, and its enrichment is associated with increased leucocyte extravasation[47,48]), serum CCL5 is not eligible as a coronary risk biomarker[46] since that CCL5 serum levels of CAD patients do not differ from those of controls (*Figure 6E*).

The CCL13/MCP-4 chemokine is a central modulator of pro-inflammatory responses acting as a pan-agonist of different chemokine receptors (i.e. CCR2, CCR3, and CCR5).[49] The deletion of CCR2 or CCR5 is associated with reduced atherosclerosis in rodents,[50–52] while CCR3 is overexpressed in human atherosclerosis and localized primarily to macrophage-rich regions of the atheroma.[53] CCL13 is also produced by other AT depots, including visceral[49] and paracardial AT,[13] and it has been suggested to positively feedback the release of other pro-atherogenic chemokines and promote atherosclerosis.[54] To test the potential of CCL13 as candidate biomarker of atherosclerosis, we then checked the levels of CCL13 protein in the systemic circulation, and we measured a significant increase in circulating CCL13 in CAD patients (*Figure 6F*). CCL13 has been described as increased also in overweight patients.[49] Since the BMI of our control group was close to normality, we could not exclude BMI as a bias for the analysis. To overcome this potential limitation, we recruited a further validation cohort of 19 overweight–obese patients referred to coronarography for one or more additional cardiovascular risk factors and chest pain, clustered on the basis of the presence/absence of CAD (characterization of this validation cohort in Supplementary Methods and Supplementary material online, *Table S1C*). Levels of CCL13 (but not of CCL5) in the serum of patients with CAD ('BMI > 25, CAD' group) were statistically increased compared with those without CAD for CCL13 (*Figure 6G* and *H*). Multiple regression analysis of the two study populations confirmed CCL13 as dependent from the presence of CAD and independent from BMI (*Figure 6I*). We thus candidate serum CCL13 as CAD biomarker, with a sensitivity of 73% and a specificity of 67% in discriminating CAD from CTRL subjects (*Figure 6J*; Cut-off of 337.7 pg/mL; area under the ROC curve 0.75). Overall, although the usefulness of CCL13 testing in predicting coronary atherosclerosis and cardiovascular events need to be validated on larger population cohorts, our results point to EAT as one of the contributors of CCL13/MCP-4 circulating levels, and to CCL13/MCP-4 as a candidate player in the pathophysiology of EAT inflammation in patients with coronary atherosclerosis, and as a putative biomarker of CAD.

3.8 miR-103-3p post-transcriptionally regulates CCL13 secretion in epicardial adipocytes

In search for miRNA likely to modulate inversely regulated mRNAs, we studied candidate mechanisms of CCL5 and CCL13 regulation. IPA 'miRNA target prediction tool' highlighted miR-103-3p (suppressed in EAT of CAD patients) as one of the candidate modulators of CCL13; this association was also predicted by other *in silico* analyses (Target Scan, miRbase, and microrna.org). miR-103-3p has been described as a key factor in adipocyte function. It is up-regulated during adipocyte differentiation and upon PPARγ activation, and suppressed

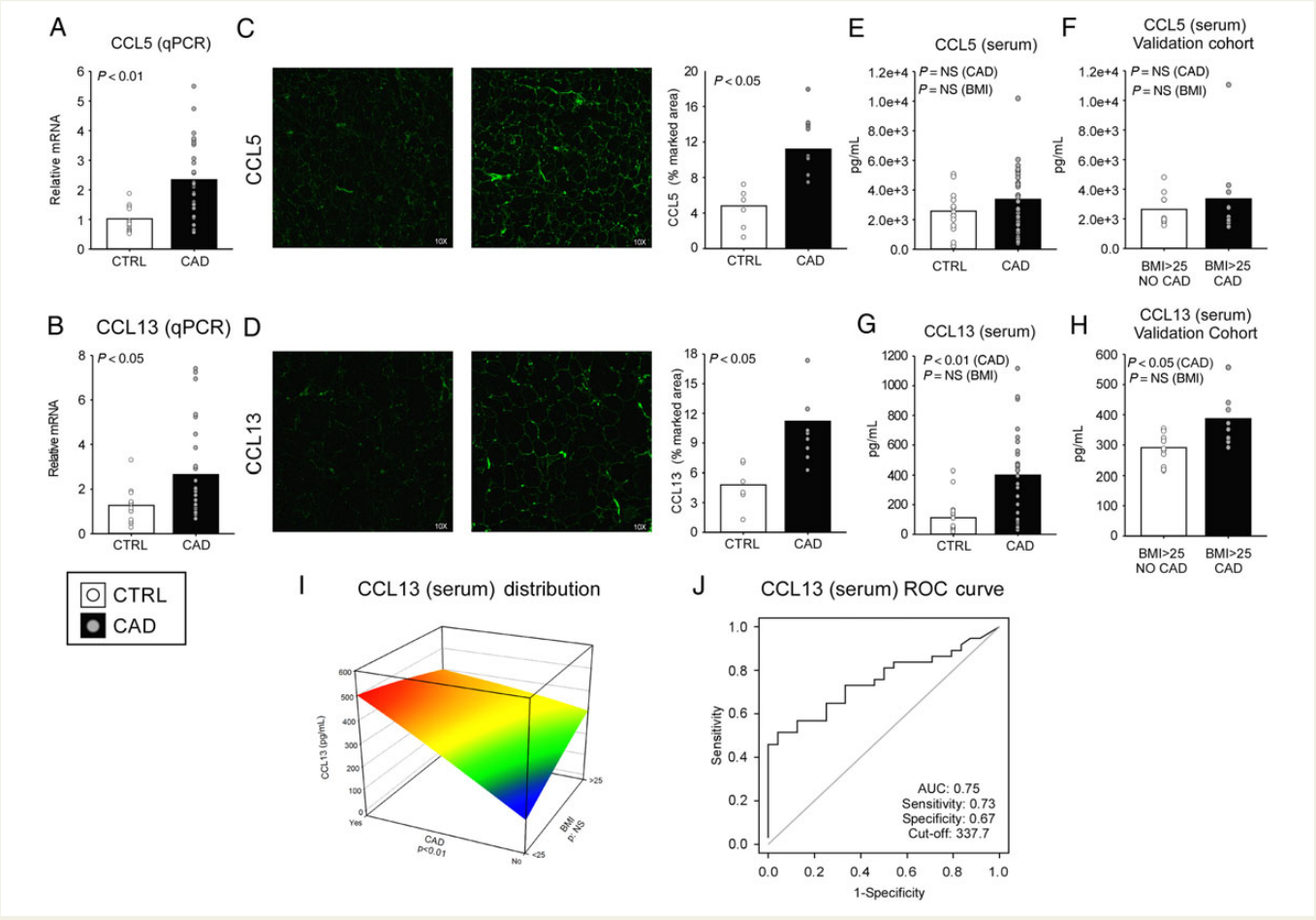

Figure 6 In CAD, EAT overexpresses CCL5 and CCL13; CCL13 may act as a candidate biomarker of CVD. RT–qPCR confirmation (13 CTRL vs. 28 CAD patients): relative mRNA expression levels of CCL5 (*A*) and CCL13 (*B*). GAPDH was used as reference gene, and values were normalized to data obtained from CTRL patients. Means are represented as bars; variability among patients is represented with a scatter plot (•: patient). Statistical significance ($P \leq 0.05$) was assessed by Mann–Whitney rank sum test. (*C* and *D*) IF (6 CTRL vs. 8 CAD patients) confirms CCL5 and CCL13 protein as increased in CAD patients (% of marked area quantified using the ImageJ software). Serum levels (quantified by ELISA kit) of CCL5 did not differ between CAD and control patients (*E* and *F*), while CCL13 is significantly increased in the CAD group both in patients undergoing cardiac surgery (14 CTRL vs. 28 CAD patients) and in the external validation cohort of patients with BMI > 25 (*G* and *H*; 10 CAD vs. 9 CAD patients). Statistical significance ($P \leq 0.05$) was assessed by the multivariate analysis keeping in consideration BMI value as a confounding factor. Modelling of CCL13 serum levels of the overall patients population (*I*; main study plus validation cohort) by multivariate analysis (25 < BMI > 25; CAD: Yes/No) and ROC curve (*J*) showing that CCL13 is a putative peripheral biomarker of CAD (area under the ROC curve: 0.75; cut-off of 337.7 pg/mL; sensitivity of 73%; specificity of 67%).

by inflammatory signals (TNFα treatment).[29,55,56] miR-103-3p has been described both down-[29] and up-regulated[56] in different animal models of obesity, unchanged in SAT of obese human subjects (see GEO repository accession numbers GSE25402[57] and GSE18470[58]), or positively correlated to BMI.[59] In our dataset of overweight CAD patients, no significant changes in miR-103-3p expression were observed in SAT (vs. CTRL; see Supplementary material online, *Figure S2A*), but we found miR-103-3p (and its host gene PANK3, see Supplementary material online, *Figure S2B*) suppressed exclusively in EAT. miR-103-3p gain of function during adipocyte differentiation has been shown to modulate insulin sensitivity[56] and adipocyte differentiation[29,56] towards the modulation of key metabolic genes such as LPL (suppressed in our database), PPARγ2 (predicted to be inhibited by IPA 'upstream regulator' analysis), and adiponectin.[29] To provide translational relevance to our observations, we thus checked the expression levels of miR-103-3p, miR-107, their hosting genes (PANK 1, 2, and 3), and CCL13 (*Figure 7A* and *B*) during a 14-day differentiation protocol of human epicardial pre-adipocytes into adipocytes (differentiation assessed by Oil Red O staining and markers of adipocyte differentiation and metabolic activity, *Figure 7C* and *D*). As previously described in mouse models,[29] miR-103-3p (with its host gene PANK3) and miR-107 (with its host gene PANK2) were induced during adipogenesis, while CCL13 was conversely suppressed. We then ectopically modulated miR-103-3p transfecting both miR-103-3p mimics and inhibitors (see Supplementary material online, *Figure S4A* and *B*; the inhibitor targeted also miR-107 as previously described[56]) in the differentiated adipocytes, and we showed that miR-103-3p was able to target CCL13 mRNA (other candidate target genes in Supplementary material online, *Figure S4B*), thus affecting CCL13 intracellular protein and secretion (*Figure 7E* and *F*). The reporter assay (CCL13 miRNA 3′UTR target sequence) confirmed CCL13 as a target of miR-103 (*Figure 7G*). The deletion of miR-103-3p target sequence (*Figure 7H*) on the 3′UTR reporter assay abolished this effect. As a result of CCL13 modulation, miR-103-3p showed anti-inflammatory

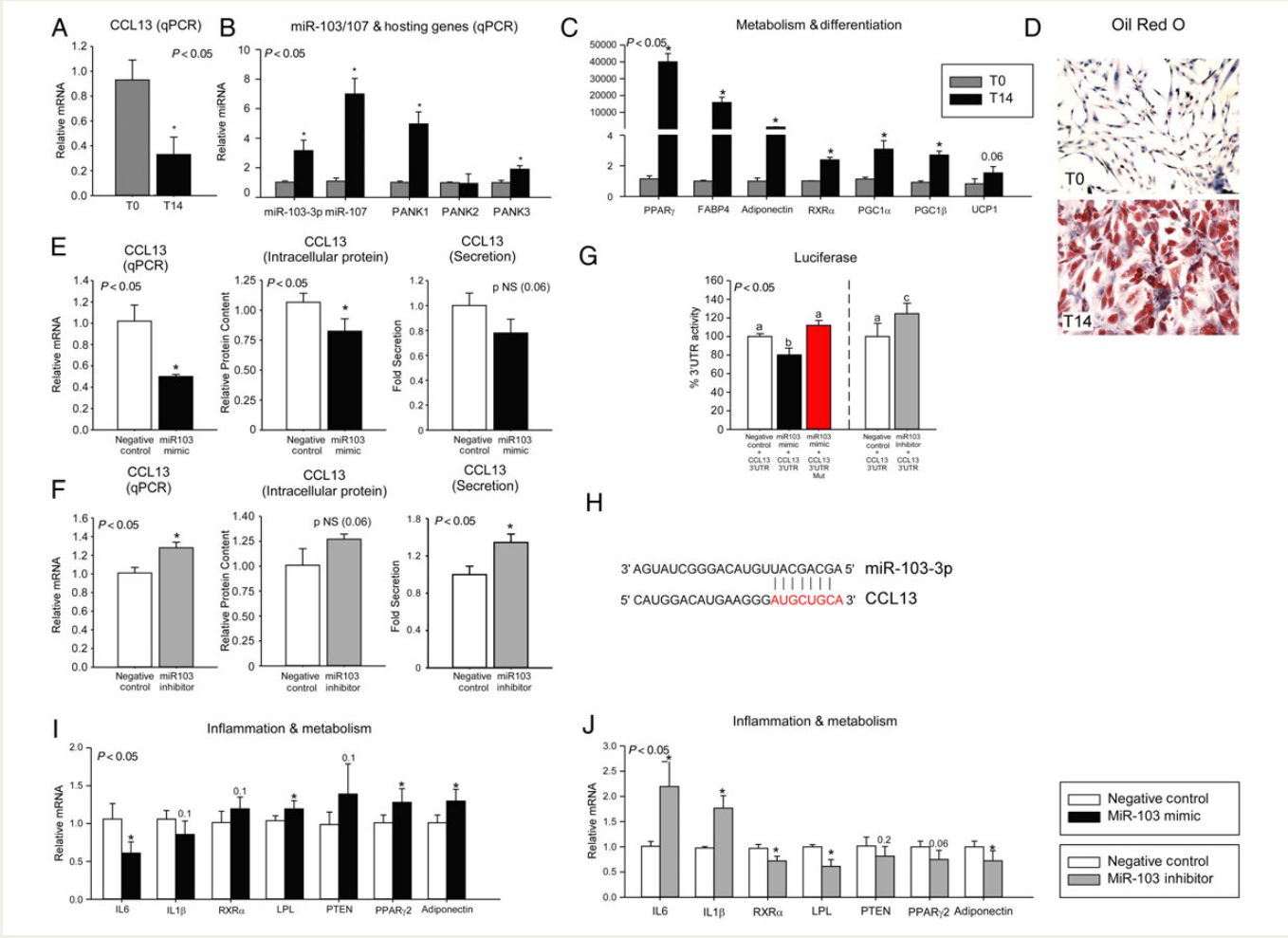

Figure 7 miR-103 modulates CCL13 in human epicardial primary adipocytes. CCL13 transcript (*A*; RT–qPCR) decreased while miR-103a-3p (with its host gene PANK3) and miR-107 (with its host gene PANK1) expression increased (*B*; RT–qPCR) in a time-dependent manner, during a 14-day differentiation protocol of human epicardial pre-adipocytes; Markers of differentiation (RT–qPCR, *C*) and Oil Red O Staining (*D*) confirmed the differentiation of preadipocytes into adipocytes. CCL13 mRNA and protein (intracellular and secreted) appeared to be differentially modulated by the transfection of miR-103 mimic (*E*) or inhibitor (*F*). In Hek293 cells (*G*), miR-103 mimic (black) and inhibitor (grey) were transfected together with a CCL13 3′UTR reporter construct, wild-type or mutated (red bar) in the miR-103 binding sequence (*H*; 'AUGCUGC' deletion in red); alterations of luciferase activity confirmed the ability of miR-103 to modulate CCL13; upon binding mutation, the modulation is lost. miR-103a-3p showed also an anti-inflammatory role (ILs) and a promotion of metabolic genes (*I*, miR-103 mimic; *J*, miR-103 inhibitor). Proteins, firefly luciferase activity, and mRNA levels were measured 48 h after transfection. To rule out unspecific effects, control cells were transfected with negative control miRNAs. U6snRNA and GAPDH were used as reference (housekeeping) for RT–qPCR, renilla luciferase activity as reference for reporter assay. Data are presented as means ± SD. Statistical significance was assessed by the Mann–Whitney rank sum test (*n*: 3; $*P \leq 0.05$) or Kruskal–Wallis tests (*n*: 3; $P \leq 0.05$; 'a', equal to reference group; 'b', different from 'a'; 'c', different from 'a' and 'b'), when appropriated.

effects (IL-6 and IL-1β); however, miR-103-3p ectopic regulation was also associated with a positive metabolic modulation, as shown by the promotion of different metabolic markers (LPL, PPARγ2, adiponectin,[29] and RXRα).

These data point to a novel role of miR-103-3p in negatively regulating inflammatory pathways and promoting adipocyte metabolism. The down-regulation of this miRNA in metabolic disease and CAD could induce a pro-inflammatory shift in EAT of patients with obesity and CAD.

4. Discussion and conclusions

The increased prevalence of obesity is a public health burden. Obesity, adiposopathy, and insulin resistance induce EAT enlargement, inflammation, and dysfunction,[1] and trigger CAD. Understanding if changes in EAT physiology are cause of atherosclerosis or just an epiphenomenon of obesity is thus mandatory. Here we provide novel information to depict the molecular identity card (genome and miRNome) of EAT (vs. SAT) in health and disease. We then present evidence that compared with SAT, EAT is characterized by enhanced inflammation and a suppression of anti-inflammatory miRNAs, supporting the concept that active inflammatory infiltrates are required for a proper EAT function.[20]

Given the close anatomic relationship between perivascular EAT and coronary arteries,[7,9] and the positive correlation between EAT and the presence of coronary atherosclerosis, our results point to EAT as a putative actor in MS/CAD. We describe that EAT in CAD displays

affected metabolic pathways with suppression of lipid- and retinoid-sensing NRs transcriptional activities, increased inflammatory infiltrates, activation of innate and adaptive immune responses with the antigen presenting pathways (MHC Class II), the enhanced communication among inflammatory cells, and chemokine signalling (CCL5, CCL13, and CCL5R) as prominent features. These genomic alterations are sustained and integrated by changes in the miRNome characterizing EAT in CAD. Our integrative analysis highlighted miR-103-3p as suppressed in EAT of CAD patients; we also showed that miR-103-3p modulation is one of the possible mechanisms (but reasonably not the exclusive) modulating CCL13/MCP-4 in EAT. Interestingly, CCL13 circulating levels are increased in CAD patients, thus highlighting this chemokine as candidate biomarker of CAD. Further experimental confirmation that the lipid-sensing NRs/miR-103-3p/CCL13 axis in EAT may be causative of CAD requires relevant animal models. Unfortunately, species differences are currently limiting this work. In mice, CCL13 is not conserved, and the lipid metabolism and EAT characteristics are very different from human. Inducing CAD in the murine model is likewise very difficult. Since changes in behaviour and NRs pharmacological modulation (e.g. TZDs) can modulate EAT physiology,[35,60] future insights are needed to develop novel strategies aimed to prevent or delay EAT enlargement, dysfunction and inflammation in obesity, and to check its consequences in CAD progression. In this respect, miR-103-3p/CCL13 might represent a novel pair of key actors of EAT dysfunction with a bona fide prognostic value in CAD.

Supplementary material

Supplementary material is available at *Cardiovascular Research* online.

Acknowledgements

The authors are indebted to P. Caldarola, M. Copetti, N. Locuratolo, R. Mariani-Costantini, R. Salvia, L. Sublimi Saponetti and all the clinicians and nurses of Policlinico 'Malpighi' of Bologna and of the 'San Paolo' Hospital of Bari for criticisms and help during the study.

Conflict of interest: none declared.

Funding

The work was funded by NR-NET FP7 Marie Curie ITN (to A.M.), Italian Ministry of University and Education (Finanziamenti per la Ricerca di Base IDEAS RBID08C9N7 to A.M.; Programma Operativo Nazionale PON01_01958 to A.M.; PRIN 2010FHH32M-002 to A.M.; PRIN 20085Y7XT5_004 to G.P.); Italian Ministry of Health (Young Researchers Grants GR-2008-1143546 and GR-2010-2314703 to A.M.); Apulian Region (POR Strategic Projects, CIP PS_101 to G.P.); University of Bari, Italy (ORBA 08WEZJ, 07X7Q1, 06BXVC, IDEA GRBA0802SJ to A.M.). M.V. is supported by the Fondazione 'Umberto Veronesi' (fellowship) and by the Medical Research Council (MRC-HNR; MC_PC_13030). M.C. is a post-doctoral fellow of AIRC.

References

1. Iacobellis G, Bianco AC. Epicardial adipose tissue: emerging physiological, pathophysiological and clinical features. *Trends Endocrinol Metab* 2011;**22**:450–457.
2. Pierdomenico SD, Pierdomenico AM, Cuccurullo F, Iacobellis G. Meta-analysis of the relation of echocardiographic epicardial adipose tissue thickness and the metabolic syndrome. *Am J Cardiol* 2013;**111**:73–78.
3. Xu Y, Cheng X, Hong K, Huang C, Wan L. How to interpret epicardial adipose tissue as a cause of coronary artery disease: a meta-analysis. *Coron Artery Dis* 2012;**23**:227–233.
4. Venteclef N, Guglielmi V, Balse E, Gaborit B, Cotillard A, Atassi F, Amour J, Leprince P, Dutour A, Clement K, Hatem SN. Human epicardial adipose tissue induces fibrosis of the atrial myocardium through the secretion of adipo-fibrokines. *Eur Heart J* 2015;**36**:795–805.
5. Mazurek T, Kiliszek M, Kobylecka M, Skubisz-Gluchowska J, Kochman J, Filipiak K, Krolicki L, Opolski G. Relation of proinflammatory activity of epicardial adipose tissue to the occurrence of atrial fibrillation. *Am J Cardiol* 2014;**113**:1505–1508.
6. Rabkin SW. Epicardial fat: properties, function and relationship to obesity. *Obes Rev* 2007;**8**:253–261.
7. Marchington JM, Mattacks CA, Pond CM. Adipose tissue in the mammalian heart and pericardium: structure, foetal development and biochemical properties. *Comp Biochem Physiol B* 1989;**94**:225–232.
8. Sacks HS, Fain JN, Bahouth SW, Ojha S, Frontini A, Budge H, Cinti S, Symonds ME. Adult epicardial fat exhibits beige features. *J Clin Endocrinol Metab* 2013;**98**:E1448–E1455.
9. Gaborit B, Venteclef N, Ancel P, Pelloux V, Gariboldi V, Leprince P, Amour J, Hatem SN, Jouve E, Dutour A, Clement K. Human epicardial adipose tissue has a specific transcriptomic signature depending on its anatomical peri-atrial, periventricular or peri-coronary location. *Cardiovasc Res* 2015;**108**:62–73.
10. Baker AR, Harte AL, Howell N, Pritlove DC, Ranasinghe AM, da Silva NF, Youssef EM, Khunti K, Davies MJ, Bonser RS, Kumar S, Pagano D, McTernan PG. Epicardial adipose tissue as a source of nuclear factor-kappaB and c-Jun N-terminal kinase mediated inflammation in patients with coronary artery disease. *J Clin Endocrinol Metab* 2009;**94**:261–267.
11. Mazurek T, Zhang L, Zalewski A, Mannion JD, Diehl JT, Arafat H, Sarov-Blat L, O'Brien S, Keiper EA, Johnson AG, Martin J, Goldstein BJ, Shi Y. Human epicardial adipose tissue is a source of inflammatory mediators. *Circulation* 2003;**108**:2460–2466.
12. McAninch EA, Fonseca TL, Poggioli R, Panos AL, Salerno TA, Deng Y, Li Y, Bianco AC, Iacobellis G. Epicardial adipose tissue has a unique transcriptome modified in severe coronary artery disease. *Obesity (Silver Spring)* 2015;**23**:1267–1278.
13. Greulich S, Maxhera B, Vandenplas G, de Wiza DH, Smiris K, Mueller H, Heinrichs J, Blumensatt M, Cuvelier C, Akhyari P, Ruige JB, Ouwens DM, Eckel J. Secretory products from epicardial adipose tissue of patients with type 2 diabetes mellitus induce cardiomyocyte dysfunction. *Circulation* 2012;**126**:2324–2334.
14. Lim LP, Lau NC, Garrett-Engele P, Grimson A, Schelter JM, Castle J, Bartel DP, Linsley PS, Johnson JM. Microarray analysis shows that some microRNAs downregulate large numbers of target mRNAs. *Nature* 2005;**433**:769–773.
15. Hilton C, Neville MJ, Karpe F. MicroRNAs in adipose tissue: their role in adipogenesis and obesity. *Int J Obes (Lond)* 2013;**37**:325–332.
16. Arner E, Mejhert N, Kulyte A, Balwierz PJ, Pachkov M, Cormont M, Lorente-Cebrian S, Ehrlund A, Laurencikiene J, Heden P, Dahlman-Wright K, Tanti JF, Hayashizaki Y, Ryden M, Dahlman I, van NE, Daub CO, Arner P. Adipose tissue microRNAs as regulators of CCL2 production in human obesity. *Diabetes* 2012;**61**:1986–1993.
17. Rottiers V, Naar AM. MicroRNAs in metabolism and metabolic disorders. *Nat Rev Mol Cell Biol* 2012;**13**:239–250.
18. Guauque-Olarte S, Gaudreault N, Piche ME, Fournier D, Mauriege P, Mathieu P, Bosse Y. The transcriptome of human epicardial, mediastinal and subcutaneous adipose tissues in men with coronary artery disease. *PLoS One* 2011;**6**:e19908.
19. Fain JN, Sacks HS, Bahouth SW, Tichansky DS, Madan AK, Cheema PS. Human epicardial adipokine messenger RNAs: comparisons of their expression in substernal, subcutaneous, and omental fat. *Metabolism* 2010;**59**:1379–1386.
20. Wernstedt AI, Tao C, Morley TS, Wang QA, Delgado-Lopez F, Wang ZV, Scherer PE. Adipocyte inflammation is essential for healthy adipose tissue expansion and remodeling. *Cell Metab* 2014;**20**:103–118.
21. Mori M, Nakagami H, Rodriguez-Araujo G, Nimura K, Kaneda Y. Essential role for miR-196a in brown adipogenesis of white fat progenitor cells. *PLoS Biol* 2012;**10**:e1001314.
22. Wang Q, Li YC, Wang J, Kong J, Qi Y, Quigg RJ, Li X. miR-17–92 cluster accelerates adipocyte differentiation by negatively regulating tumor-suppressor Rb2/p130. *Proc Natl Acad Sci USA* 2008;**105**:2889–2894.
23. Fang Y, Shi C, Manduchi E, Civelek M, Davies PF. MicroRNA-10a regulation of proinflammatory phenotype in athero-susceptible endothelium in vivo and in vitro. *Proc Natl Acad Sci USA* 2010;**107**:13450–13455.
24. Garg M, Potter JA, Abrahams VM. Identification of microRNAs that regulate TLR2-mediated trophoblast apoptosis and inhibition of IL-6 mRNA. *PLoS One* 2013;**8**:e77249.
25. Halappanavar S, Nikota J, Wu D, Williams A, Yauk CL, Stampfli M. IL-1 receptor regulates microRNA-135b expression in a negative feedback mechanism during cigarette smoke-induced inflammation. *J Immunol* 2013;**190**:3679–3686.
26. Xie T, Liang J, Liu N, Wang Q, Li Y, Noble PW, Jiang D. MicroRNA-127 inhibits lung inflammation by targeting IgG Fcgamma receptor I. *J Immunol* 2012;**188**:2437–2444.
27. Walden TB, Timmons JA, Keller P, Nedergaard J, Cannon B. Distinct expression of muscle-specific microRNAs (myomirs) in brown adipocytes. *J Cell Physiol* 2009;**218**:444–449.
28. Belarbi Y, Mejhert N, Lorente-Cebrian S, Dahlman I, Arner P, Ryden M, Kulyte A. MicroRNA-193b controls adiponectin production in human white adipose tissue. *J Clin Endocrinol Metab* 2015;**100**:E1084–1088.
29. Xie H, Lim B, Lodish HF. MicroRNAs induced during adipogenesis that accelerate fat cell development are downregulated in obesity. *Diabetes* 2009;**58**:1050–1057.

30. Zaragosi LE, Wdziekonski B, Brigand KL, Villageois P, Mari B, Waldmann R, Dani C, Barbry P. Small RNA sequencing reveals miR-642a-3p as a novel adipocyte-specific microRNA and miR-30 as a key regulator of human adipogenesis. *Genome Biol* 2011;**12**: R64.
31. Chartoumpekis DV, Zaravinos A, Ziros PG, Iskrenova RP, Psyrogiannis AI, Kyriazopoulou VE, Habeos IG. Differential expression of microRNAs in adipose tissue after long-term high-fat diet-induced obesity in mice. *PLoS One* 2012;**7**:e34872.
32. Schoonjans K, Staels B, Auwerx J. Role of the peroxisome proliferator-activated receptor (PPAR) in mediating the effects of fibrates and fatty acids on gene expression. *J Lipid Res* 1996;**37**:907–925.
33. Zhang Y, Repa JJ, Gauthier K, Mangelsdorf DJ. Regulation of lipoprotein lipase by the oxysterol receptors, LXRalpha and LXRbeta. *J Biol Chem* 2001;**276**:43018–43024.
34. John E, Wienecke-Baldacchino A, Liivrand M, Heinaniemi M, Carlberg C, Sinkkonen L. Dataset integration identifies transcriptional regulation of microRNA genes by PPAR-gamma in differentiating mouse 3T3-L1 adipocytes. *Nucleic Acids Res* 2012;**40**: 4446–4460.
35. Sacks HS, Fain JN, Cheema P, Bahouth SW, Garrett E, Wolf RY, Wolford D, Samaha J. Inflammatory genes in epicardial fat contiguous with coronary atherosclerosis in the metabolic syndrome and type 2 diabetes: changes associated with pioglitazone. *Diabetes Care* 2011;**34**:730–733.
36. Shulman AI, Mangelsdorf DJ. Retinoid x receptor heterodimers in the metabolic syndrome. *N Engl J Med* 2005;**353**:604–615.
37. Dozio E, Vianello E, Briganti S, Fink B, Malavazos AE, Scognamiglio ET, Dogliotti G, Sigruener A, Schmitz G, Corsi Romanelli MM. Increased reactive oxygen species production in epicardial adipose tissues from coronary artery disease patients is associated with brown-to-white adipocyte trans-differentiation. *Int J Cardiol* 2014;**174**:413–414.
38. Hruskova Z, Biswas SK. A new "immunological" role for adipocytes in obesity. *Cell Metab* 2013;**17**:315–317.
39. Deng T, Lyon CJ, Minze LJ, Lin J, Zou J, Liu JZ, Ren Y, Yin Z, Hamilton DJ, Reardon PR, Sherman V, Wang HY, Phillips KJ, Webb P, Wong ST, Wang RF, Hsueh WA. Class II major histocompatibility complex plays an essential role in obesity-induced adipose inflammation. *Cell Metab* 2013;**17**:411–422.
40. Cho KW, Morris DL, DelProposto JL, Geletka L, Zamarron B, Martinez-Santibanez G, Meyer KA, Singer K, O'Rourke RW, Lumeng CN. An MHC II-dependent activation loop between adipose tissue macrophages and CD4+ T cells controls obesity-induced inflammation. *Cell Rep* 2014;**9**:605–617.
41. Hansson GK. Inflammation, atherosclerosis, and coronary artery disease. *N Engl J Med* 2005;**352**:1685–1695.
42. Shimabukuro M, Hirata Y, Tabata M, Dagvasumberel M, Sato H, Kurobe H, Fukuda D, Soeki T, Kitagawa T, Takanashi S, Sata M. Epicardial adipose tissue volume and adipocytokine imbalance are strongly linked to human coronary atherosclerosis. *Arterioscler Thromb Vasc Biol* 2013;**33**:1077–1084.
43. Hirata Y, Tabata M, Kurobe H, Motoki T, Akaike M, Nishio C, Higashida M, Mikasa H, Nakaya Y, Takanashi S, Igarashi T, Kitagawa T, Sata M. Coronary atherosclerosis is associated with macrophage polarization in epicardial adipose tissue. *J Am Coll Cardiol* 2011;**58**:248–255.
44. Verhagen SN, Vink A, van der Graaf Y, Visseren FL. Coronary perivascular adipose tissue characteristics are related to atherosclerotic plaque size and composition. A post-mortem study. *Atherosclerosis* 2012;**225**:99–104.
45. Madani R, Karastergiou K, Ogston NC, Miheisi N, Bhome R, Haloob N, Tan GD, Karpe F, Malone-Lee J, Hashemi M, Jahangiri M, Mohamed-Ali V. RANTES release by human adipose tissue in vivo and evidence for depot-specific differences. *Am J Physiol Endocrinol Metab* 2009;**296**:E1262–E1268.
46. Herder C, Peeters W, Illig T, Baumert J, de Kleijn DP, Moll FL, Poschen U, Klopp N, Muller-Nurasyid M, Roden M, Preuss M, Karakas M, Meisinger C, Thorand B, Pasterkamp G, Koenig W, Assimes TL, Deloukas P, Erdmann J, Holm H, Kathiresan S, Konig IR, McPherson R, Reilly MP, Roberts R, Samani NJ, Schunkert H, Stewart AF. RANTES/CCL5 and risk for coronary events: results from the MONICA/KORA Augsburg case-cohort, Athero-Express and CARDIoGRAM studies. *PLoS One* 2011;**6**:e25734.
47. von HP, Weber KS, Huo Y, Proudfoot AE, Nelson PJ, Ley K, Weber C. RANTES deposition by platelets triggers monocyte arrest on inflamed and atherosclerotic endothelium. *Circulation* 2001;**103**:1772–1777.
48. von HP, Koenen RR, Sack M, Mause SF, Adriaens W, Proudfoot AE, Hackeng TM, Weber C. Heterophilic interactions of platelet factor 4 and RANTES promote monocyte arrest on endothelium. *Blood* 2005;**105**:924–930.
49. Hashimoto I, Wada J, Hida A, Baba M, Miyatake N, Eguchi J, Shikata K, Makino H. Elevated serum monocyte chemoattractant protein-4 and chronic inflammation in overweight subjects. *Obesity (Silver Spring)* 2006;**14**:799–811.
50. Braunersreuther V, Zernecke A, Arnaud C, Liehn EA, Steffens S, Shagdarsuren E, Bidzhekov K, Burger F, Pelli G, Luckow B, Mach F, Weber C. Ccr5 but not Ccr1 deficiency reduces development of diet-induced atherosclerosis in mice. *Arterioscler Thromb Vasc Biol* 2007;**27**:373–379.
51. Martinez HG, Quinones MP, Jimenez F, Estrada CA, Clark K, Muscogiuri G, Sorice G, Musi N, Reddick RL, Ahuja SS. Critical role of chemokine (C-C motif) receptor 2 (CCR2) in the KKAy + Apoe -/- mouse model of the metabolic syndrome. *Diabetologia* 2011;**54**:2660–2668.
52. Veillard NR, Kwak B, Pelli G, Mulhaupt F, James RW, Proudfoot AE, Mach F. Antagonism of RANTES receptors reduces atherosclerotic plaque formation in mice. *Circ Res* 2004; **94**:253–261.
53. Haley KJ, Lilly CM, Yang JH, Feng Y, Kennedy SP, Turi TG, Thompson JF, Sukhova GH, Libby P, Lee RT. Overexpression of eotaxin and the CCR3 receptor in human atherosclerosis: using genomic technology to identify a potential novel pathway of vascular inflammation. *Circulation* 2000;**102**:2185–2189.
54. Breland UM, Michelsen AE, Skjelland M, Folkersen L, Krohg-Sorensen K, Russell D, Ueland T, Yndestad A, Paulsson-Berne G, Damas JK, Oie E, Hansson GK, Halvorsen B, Aukrust P. Raised MCP-4 levels in symptomatic carotid atherosclerosis: an inflammatory link between platelet and monocyte activation. *Cardiovasc Res* 2010; **86**:265–273.
55. Sun T, Fu M, Bookout AL, Kliewer SA, Mangelsdorf DJ. MicroRNA let-7 regulates 3T3-L1 adipogenesis. *Mol Endocrinol* 2009;**23**:925–931.
56. Trajkovski M, Hausser J, Soutschek J, Bhat B, Akin A, Zavolan M, Heim MH, Stoffel M. MicroRNAs 103 and 107 regulate insulin sensitivity. *Nature* 2011;**474**:649–653.
57. Neville MJ, Collins JM, Gloyn AL, McCarthy MI, Karpe F. Comprehensive human adipose tissue mRNA and microRNA endogenous control selection for quantitative real-time-PCR normalization. *Obesity (Silver Spring)* 2011;**19**:888–892.
58. Ortega FJ, Moreno-Navarrete JM, Pardo G, Sabater M, Hummel M, Ferrer A, Rodriguez-Hermosa JI, Ruiz B, Ricart W, Peral B, Fernandez-Real JM. MiRNA expression profile of human subcutaneous adipose and during adipocyte differentiation. *PLoS One* 2010;**5**:e9022.
59. Bork-Jensen J, Thuesen AC, Bang-Bertelsen CH, Grunnet LG, Pociot F, Beck-Nielsen H, Ozanne SE, Poulsen P, Vaag A. Genetic versus non-genetic regulation of miR-103, miR-143 and miR-483–3p expression in adipose tissue and their metabolic implications-A twin study. *Genes (Basel)* 2014;**5**:508–517.
60. Company JM, Booth FW, Laughlin MH, Arce-Esquivel AA, Sacks HS, Bahouth SW, Fain JN. Epicardial fat gene expression after aerobic exercise training in pigs with coronary atherosclerosis: relationship to visceral and subcutaneous fat. *J Appl Physiol* 2010; **109**:1904–1912.